Nonlinear planar optical waveguide sensor loaded with metamaterials

WENWEI NIU, MING HUANG*, ZHE XIAO[a], JINGJING YANG
School of Information Science and Engineering, Yunnan University, Kunming 650091, PR China
[a]School of Electrical & Electronic Engineering, Nanyang Technological University, Western Catchment Area 639798, Singapore

Metamaterials are artificial multifunctional materials that gain its material properties from its structure rather than inheriting them directly from the materials it is composed of, and it may provide novel tools to significantly enhance the sensitivity and resolution of the sensors. In this paper, we present a nonlinear planar optical waveguide sensor loaded with a metamaterial layer. The dispersion relation of the waveguide is theoretically derived, and we compute the field distribution for the proposed sensor, and find that the field intensity is enhanced comparing with that without metamaterials. We compute the sensitivity and the fraction of total power flowing in the cladding, and investigate the influence of various parameters of the sensor on its sensitivity. Compared to the traditional nonlinear planar optical waveguide sensor, the maximum sensitivity of proposed sensor is 2.167 times for TE mode, and 2.335 times for TM mode. Compared to the metamaterial assisted linear planar optical waveguide sensor, the maximum sensitivity of proposed sensor is 1.167 times for TE mode; For TM mode, the sensitivity of proposed sensor is much higher when increasing the thickness of the guiding layer. It might open a door for designing sensors with specified sensitivity.

(Received August 26, 2011; accepted October 20, 2011)

Keywords: Optical sensor, Metamaterials, Nonlinear, Sensitivity, Evanescent field

1. Introduction

Processes involving the interaction between light and matter are fundamental to much of science [1]. Optical sensors based on the interaction of evanescent field with surrounding medium have recently sparked enormous interests in different sensing applications [2-6]. A vast variety of sensing mechanisms have been proposed, including whispering-gallery-mode [7], reverse symmetry waveguide [8], surface plasmon resonance [9], Michelson interferometers [10], photonic crystal [11], fiber Bragg grating [12], Raman scattering [13], etc. Among these, optical waveguide sensor, which is based on measuring measurand-induced changes of refractive, absorptive or luminescent properties of a medium or of a layer located in the evanescent wave region of the propagating mode [14], is beneficial to use to achieve high sensitivity, fast response time, remote controllability, system compactness, and intrinsically safe detection, little or no inference in the waveguide element, and low cost [15]. Thus, various optical waveguide sensors have been proposed [16-19]. Efforts to improve the sensitivity of optical waveguide sensors have attracted interests. Researches have shown that evanescent wave amplification by metamaterials [20] and nonlinearity medium could improve the sensitivity of the optical waveguide sensor. For example, Taya et al. [21] showed that the sensitivity of an optical waveguide sensor can be dramatically enhanced by using metamaterials with negative permittivity and permeability. Niu et al. [22] investigated the dispersion equation of the linear planar optical waveguide with metamaterial layer for TM mode, and showed that this sensor can dramatically enhance the sensitivity compared with the linear planar waveguide sensors without metamaterials for TM mode and the sensor for TE mode developed in [21]. In the case of homogeneous sensing, the sensitivity of a nonlinear three-layer slab waveguide optical sensor can be improved by using nonlinear cladding and substrate was shown by Taya et al. [23]. Kumar et al. [24] demonstrated that the sensitivity of a nonlinear asymmetrical metal-clad planar waveguide sensor was improved by introducing a nonlinear material in the cover medium. Our group showed that the sensitivity of a nonlinear planar optical waveguide with metamaterials for TE mode can be enhanced compared with that without metamaterials and the linear planar optical waveguide sensor with metamaterials [25]. However, to the best of our knowledge, there is no report for sensing applications of the nonlinear planar optical waveguide with metamaterials for TM mode.

In this paper, we present a theoretical analysis of a planar waveguide sensor loaded with metamaterials based on nonlinear cladding and substrate which are two Kerr type nonlinear media. We investigate the influences of different parameters of the proposed sensor on the sensitivity, including geometry parameters, transmission

mode and dielectric characteristics of the waveguide. We show that the proposed sensor could be used to improve the performance of the sensitivity drastically compared with other sensors by proper selection of structure parameters.

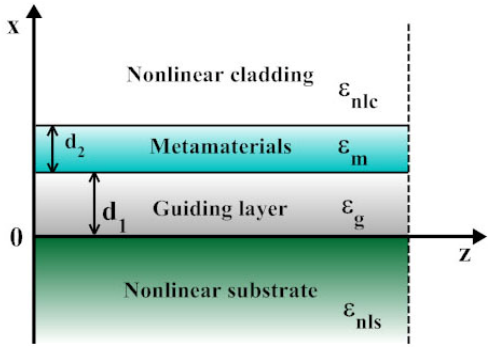

Fig. 1. Schematic diagram of a cross sectional view of the nonlinear planar waveguide sensor with a metamaterial layer.

2. Theory analysis

The schematic diagram of a four-layered waveguide sensor model is illustrated in Fig. 1. It is taken to be infinite in extent in both the z and y direction. There are four layers in the waveguide, from the top to the bottom which are semi-infinite nonlinear cladding, metamaterial layer, guiding layer and semi-infinite nonlinear substrate, respectively. The geometry parameters of the waveguide include the guiding layer thickness d_1, the metamaterial thickness d_2. Permittivities for the four layers are ε_{nlc}, ε_m, ε_g and ε_{nls}, respectively. The nonlinear cladding and substrate are supposed to be of Kerr type, and their dielectric functions can be written as [23]: $\varepsilon_{nlc} = \varepsilon_c + \alpha_c^{'} \left|H_{yc}\right|^2$ and $\varepsilon_{nls} = \varepsilon_s + \alpha_s^{'} \left|H_{ys}\right|^2$, where $\alpha_c^{'} = \alpha_c / \varepsilon_c \mathrm{c}^2 \varepsilon_0^2$ and $\alpha_s^{'} = \alpha_s / \varepsilon_s c^2 \varepsilon_0^2$ are the nonlinear coefficients of the cladding and substrate, ε_c and ε_s are the linear parts of the permittivities, H_{yc} and H_{ys} are the magnetic field intensity in cladding and substrate, respectively.

In the waveguide structure, the fields of the *p*-polarized waves (TM mode ($\boldsymbol{E}\{E_x, 0, E_z\}$, $\boldsymbol{H}\{0, H_y, 0\}$)) propagate along the z-direction. The required magnetic fields in each layer are:

$$H_{yc} = \sqrt{2/\alpha_c} q_c \operatorname{sech}(k_0 q_c (x - x_c)), \qquad x > d_1 + d_2, \tag{1}$$

$$H_{ym} = D_1 \exp(-k_0 q_m x) + D_2 \exp(k_0 q_m x), d_1 < x < d_1 + d_2, \tag{2}$$

$$H_{yg} = A\cos(k_0 q_g x) + B\sin(k_0 q_g x), \qquad 0 < x < d_1, \tag{3}$$

$$H_{ys} = \sqrt{2/\alpha_s} q_s \operatorname{sech}(k_0 q_s (x_s - x)), \qquad x < 0, \tag{4}$$

where $q_c = \sqrt{N^2 - \varepsilon_c}$, $q_m = \sqrt{N^2 - n\varepsilon_m}$, $q_g = \sqrt{\varepsilon_g - N^2}$ and $q_s = \sqrt{N^2 - \varepsilon_s}$, n is a negative number ($n = \mu_m / \mu_0$, μ_m is the permeability of the metamaterials, μ_0 is the permeability of vacuum), N is the effective refractive index, x_c and x_s are constants related to the field distribution in the cladding and substrate, A, B and D_1, D_2 are the unknown constants and determined from the boundary conditions. As a result of matching the fields H_y and $E_z(x) = (1/\mathrm{j}\omega\varepsilon(x))(\partial H_y(x)/\partial x)$ to be continuous at x=0, d_1 and d_1+d_2. After algebraic operation, the dispersion relations of the proposed waveguide can be obtained:

$$k_0 q_g d_1 = \arctan\left(\frac{q_m \varepsilon_g}{q_g \varepsilon_m}\left(\frac{(q_m \varepsilon_c + q_c \varepsilon_m \tanh C) - (q_m \varepsilon_c - q_c \varepsilon_m \tanh C)\exp(-2k_0 q_m d_2)}{(q_m \varepsilon_c + q_c \varepsilon_m \tanh C) + (q_m \varepsilon_c - q_c \varepsilon_m \tanh C)\exp(-2k_0 q_m d_2)}\right)\right)$$
$$+ \arctan\left(\frac{q_s \varepsilon_g}{q_g \varepsilon_s} \tanh C_s\right) + m\pi, \tag{5}$$

where k_0 is the free space wave number, $C_s = k_0 q_s x_s$ is the substrate guiding interface nonlinearity, $C_c = k_0 q_c (d_1 - x_c)$ is the cladding guiding interface nonlinearity, and $C = k_0 q_c (d_1 + d_2 - x_c) = C_c + k_0 q_c d_2$, m = 0, 1, 2...is the mode order.

According to Eqs. (1)-(5), the distribution of normalized magnetic field can be computed, as shown in Fig. 2. It is assumed that parameters of the waveguide without metamaterials are d_1=500 nm, ε_c= 2, ε_s = 2.2, ε_g = 4 and λ=1550 nm. For the waveguide sensor loaded with a layer of metamaterials, parameters are set to be d_1=500 nm, ε_c =2, ε_s =2.2, ε_g=4, ε_m =-2, d_2=80 nm, n=-0.6 and λ=1550 nm. It is obvious that there is a sharp increase of evanescent field in the guiding layer, metamaterial layer and cladding. The magnetic field intensity at the surface of the metamaterial layer is about 2.46 times that of the waveguide without a metamaterial layer. Similar to the above procedure, the magnetic field intensity for the TE mode waveguide loaded with a layer of metamaterials can also be calculated, and the amplification is about 2.76 times that of the waveguide without metamaterials. Therefore, metamaterials can be used to improve the sensitivity of the optical sensor, since the amplification of evanescent field.

When d_2 approaches zero, Eq. (5) can be reduced to

$$k_0 q_g d_1 = \arctan(X_s / a_s \tanh C_s) + \arctan(X_c / a_c \tanh C_c) + m\pi, \tag{6}$$

This is a well-known three-layer nonlinear waveguide dispersion relation [23].

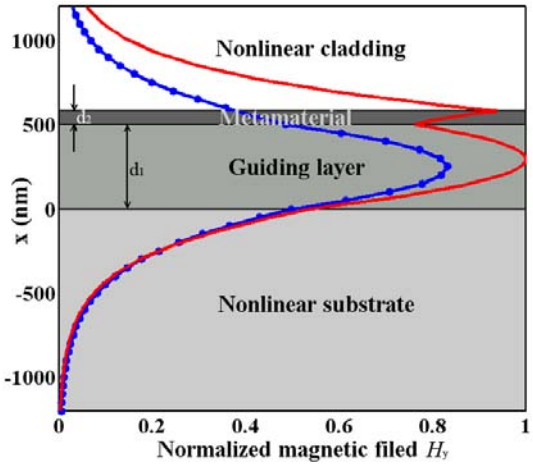

Fig. 2. Normalized magnetic field H_y distribution along the x-direction in nonlinear planar waveguide sensor without (dotted blue line) and with a metamaterial layer (solid red line), the horizontal lines denote the interfaces of two layers.

Let three normalized effective indices X_s, X_c, and X_m and three asymmetry parameters a_s, a_c, and a_m be $X_s = q_s/q_g$, $X_c = q_c/q_g$, $X_m = q_m/q_g$, $a_s = \varepsilon_s/\varepsilon_g$, $a_c = \varepsilon_c/\varepsilon_g$, and $a_m = \varepsilon_m/\varepsilon_g$. In addition, q_g, X_c, the effective refractive index N can be written as a function of X_s:

$$q_g = \sqrt{\varepsilon_g}\sqrt{(1-a_s)/(1+X_s^2)},$$

$$X_c^2 = (1-a_c)(1+X_s^2)/(1-a_s) - 1,$$

$$N = \sqrt{\varepsilon_g}\sqrt{(a_s + X_s^2)/(1+X_s^2)}.$$

Then, Eq. (5) becomes

$$k_0 q_g d_1 = \arctan(X_s/a_s \tanh C_s) + \arctan(X_m b_1/(a_m b_2)) + m\pi, \quad (7)$$

where

$$b_1 = (a_c X_m + a_m X_c \tanh C) - (a_c X_m - a_m X_c \tanh C) \exp(-2k_0 X_m q_g d_2), \quad b_2 = (a_c X_m + a_m X_c \tanh C) + (a_c X_m - a_m X_c \tanh C) \exp(-2k_0 X_m q_g d_2).$$

In the case of homogeneous sensing, the sensing mechanism of our sensor is the rate of change of the modal effective index N under an index change of the cladding n_c i.e., $S_m = (\partial N / \partial n_c)$, where N is the modal effective refractive index, n_c is the refractive index of the cladding. By differentiating Eq. (7) with respect to N and n_c, the sensitivity of the sensor can be deduced as:

$$S_m = \frac{\sqrt{a_c}\sqrt{1+X_c^2}X_m[(R_1+R_2)(b_1+b_2)\exp(-f) - (R_1-R_2)(b_2-b_1)]}{X_c\sqrt{a_c+X_c^2}\left((A_{TM}+G_{sTM})(a_m b_2^2 + X_m^2 b_1^2/a_m) + G_1 + G_2 + b_1 b_2 C_1/X_m\right)}, \quad (8)$$

where $f = 2k_0 X_m q_g d_2$, $C_1 = 1 + X_m^2$, $C_2 = 1 + X_c^2$,

$H = k_0(d_1 + d_2 - x_c)X_c\sqrt{\varepsilon_g}\sqrt{(1-a_c)/(1+X_c^2)}(1-\tanh^2 C)$,

$H_s = k_0 x_s X_s \sqrt{\varepsilon_g}\sqrt{(1-a_s)/(1+X_s^2)}(1-\tanh^2 C_s)$, $R_1 = 2X_c X_m (1-a_c)/(1+X_c^2)$, $R_2 = a_m(\tanh C + H)$, $G_{sTM} = (a_s H_s + a_s \tanh C_s(1+X_s^2))/(X_s(a_s^2 + X_s^2 \tanh^2 C_s))$, $G_1 = (b_2 - b_1)(a_c C_1 + a_m X_m(C_2 \tanh C + H)/X_c)$, $G_2 = \exp(-f)(b_1 + b_2)((a_c X_m - a_m X_c \tanh C)f/X_m - a_c C_1 + a_m X_m(C_2 \tanh C + H)/X_c)$,

$A_{TM} = \arctan(X_s/a_s \tanh C_s) + \arctan(X_m b_1/(a_m b_2)) + m\pi$.

In addition to the theoretical sensitivity (Eq.(8)), the fraction of total power flowing in the cladding P_c/P_t is an important parameter for optical waveguide sensor. Here, P_c is the power flowing in the cladding layer, P_t is the total power flowing. Generally speaking, increasing the power flowing in the cladding layer will enhance the sensitivity of the sensor [8]. The fraction of total power flowing in the cladding can be calculated according to Poynting's theorem, and be written as:

$$P_c/P_t = P_c/(P_c + P_m + P_g + P_s) \quad (9)$$

where P_m, P_g and P_s are the power flowing in the metamaterial layer, guiding layer and substrate, and $P_c = Nk_0/(2\omega\varepsilon_c)((2/\alpha_c)(q_c/k_0)(1-\tanh C))$,

$P_m = Nk_0/(2\omega\varepsilon_m)(-D_1^2(\exp(-2k_0 q_m(d_1+d_2)) - \exp(-2k_0 q_m d_1))/(2k_0 q_m) + 2D_1 D_2 d_2 + D_2^2(\exp(2k_0 q_m(d_1+d_2)) - \exp(2k_0 q_m d_1))/(2k_0 q_m))$,

$P_g = Nk_0/(2\omega\varepsilon_g)(d_1(A^2+B^2)/2 + \sin(2k_0 q_g d_1)(A^2 - B^2)/(4k_0 q_g) + AB(1-\cos(2k_0 q_g d_1))/(2k_0 q_g))$,

$P_s = Nk_0/(2\omega\varepsilon_s)((2/\alpha_s)(q_s/k_0)(1-\tanh C_s))$.

where $A = \sqrt{2/\alpha_s}\, q_s \operatorname{sech} C_s$, $B = X_s/a_s\sqrt{2/\alpha_s}\, q_s \tanh C_s \operatorname{sech} C_s$,

$D_1 = 0.5\exp(k_0 q_m d_1)((A - a_m B/X_m)\cos(k_0 q_g d_1) + (B + a_m A/X_m)\sin(k_0 q_g d_1))$,

$D_2 = 0.5\exp(-k_0 q_m d_1)((A + a_m B/X_m)\cos(k_0 q_g d_1) + (B - a_m A/X_m)\sin(k_0 q_g d_1))$.

3. Numerical results and discussion

In the following simulation, we assume that the guiding layer of the waveguide is made of silicon nitride (Si_3N_4, n_g=2) which is a high index material, the free space wavelength λ is 1550 nm, tanhC_c = 0.6, tanhC_s = 0.7, and only fundamental mode (m=0) which is under normal circumstances since it has the highest sensitivity [21].

Fig. 3 shows the S_m and P_c/P_t as a function of guiding layer thickness d_1. It verifies the close connection between S_m and P_c/P_t, the curve trend of S_m-d_1 is compatible with that of P_c/P_t-d_1. In the case of normal symmetry (a_s>a_c), both the S_m and P_c/P_t have a peak at a specific value d_1, which we call the optimum value of guiding layer thickness, and the peak values are 0.27 and 0.38, respectively. Then the sensitivity decreases with further increasing of d_1. At small values of d_1 near cutoff thickness, the sensitivity approaches zero since the effective refractive index is close to the refractive index of the substrate and the evanescent field in the substrate is very large, resulting in the fraction of power flowing in the cladding vanishes. At relatively very high values of d_1, the sensitivity again approaches zero again due to for increased guiding layer thickness high confinement of the field within the guiding layer and thus a low power flowing in the cladding. While in the case of reverse symmetry (a_s<a_c), the sensitivity decreases with increasing d_1, the maximum sensitivity value goes to 0.55, which appears at the cutoff thicknesses, and the maximum P_c/P_t is 0.66, because it has the advantage of deeper penetration of the evanescent field into the cover medium, theoretically permitting higher sensitivity to analytes compared to traditional waveguide designs. The reverse symmetry produces an evanescent field that can penetrate deeper by reversing the mode profile, and allows for a larger part of the electromagnetic field of the guided wave to be present in the cover medium, thus enhancing the optical response to analytes compared to normal symmetry waveguides [26].

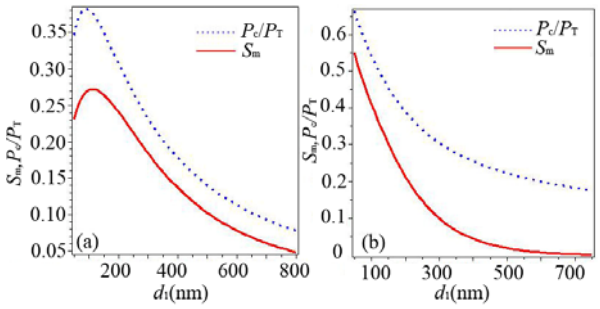

Fig. 3. Sensitivity S_m, P_c/P_t versus the guiding layer thickness d_1 for the proposed sensor (a_m=-0.5, n=-0.6, and d_2=80nm): (a) normal symmetry (a_s=0.65, a_c=0.55) (b) reverse symmetry (a_s=0.55, a_c=0.65).

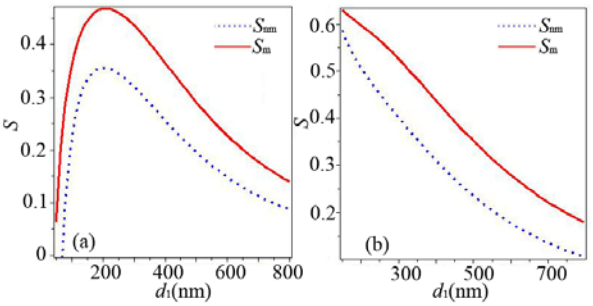

Fig. 4. Sensitivity versus the guiding layer thickness d_1 for the proposed sensor (a_m=-0.5, n=-0.6, d_2=30nm) with a metamaterial layer (red solid line) and without a metamaterial layer (blue dotted line): (a) normal symmetry (a_s = 0.55, a_c = 0.5) (b) reverse symmetry (a_s=0.5, a_c=0.55).

To compare the sensitivity of the waveguide sensor with metamaterials (S_m) and without metamaterials (S_{nm}), we plot the sensitivity S_m and S_{nm} as a function of d_1 for the waveguide in normal symmetry and reverse symmetry, as shown in Fig. 4. In the case of normal symmetry, it is observed that initially the sensitivity increases very rapidly with increasing guiding layer thickness d_1 and then it decreases with larger guiding layer thickness. The maximum sensitivity value for S_{nm} is 0.35 and for S_m is 0.46. In the case of reverse symmetry, the sensitivity curves decrease monotonously with increasing d_1, the maximum sensitivity value for S_{nm} is 0.6, while for S_m is 0.63. Thus, metamaterials can improve the sensitivity of the sensor, and the optical waveguide with metamaterials in reverse symmetry mode has much higher sensitivity.

For TM and TE mode, the sensitivity of the proposed sensor as a function of d_1 is simulated and illustrated in Fig. 5. In the case of normal symmetry shown in Fig. 5(a), an optimal guiding layer thickness is observed at around 60 nm for TE mode, while an optimal guiding layer thickness is observed at around 220 nm for TM mode. In the case of reverse symmetry shown in Fig. 5(b), the maximum sensitivity is about 0.55 for TE mode, while the maximum sensitivity is about 0.7 for TM mode. Comparing Fig. 5(a) with Fig. 5(b), we can find that the sensor in TM mode possesses higher sensitivity than that in TE mode when the guiding layer is thick enough. Besides, the maximum sensitivity of the sensor with reverse symmetry is much higher than that with normal symmetry. Therefore, the sensor for TM mode is far more sensitive than that for TE mode, the waveguide sensor in reverse symmetry configuration in TM mode is recommended.

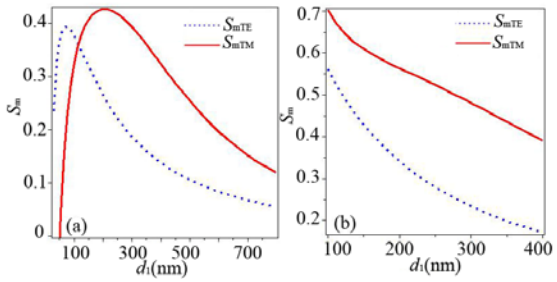

Fig. 5. Sensitivity versus the guiding layer thickness d_1 for TM mode (S_{mTM}) (red solid line) and TE mode (S_{mTE}) (blue dotted line) (d_2=20 nm, a_m=-0.5, n=-0.6): (a) normal symmetry (a_s = 0.55 and a_c = 0.5) (b) reverse symmetry (a_s = 0.5 and a_c = 0.55).

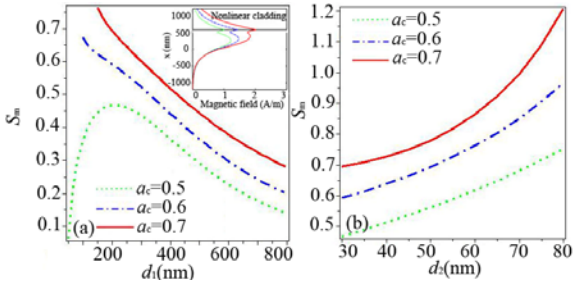

Fig. 6. (a) Sensitivity versus d_1 (d_2=30nm, a_s = 0.55, a_m=-0.5, n=-0.6); (b) Sensitivity versus d_2 (d_1=200 nm a_s = 0.55, a_m=-0.5, n=-0.6).

In order better to study the influence of dielectric characteristics and nonlinear parameters of the waveguide on the sensitivity, we simulated the sensitivity as a function of d_1, d_2, tanhC_s, tanhC_c, tanh$C$, N, and a_m for different value of a_c, as a function of d_1 for different λ as shown in Fig. 6-10. See Fig. 6 (a), in the case of normal symmetry (a_c=0.5, a_s =0.55), there is a peak on the curve S_m-d_1, while in the case of reverse symmetry (a_c=0.6, 0.7, a_s=0.55), S_m decreases monotonously with increasing d_1. This is also verified by the inset of magnetic field distribution in Fig. 6(a). The curves of S_m as a function of metamaterial thickness d_2 in Fig. 6 (b) show that S_m increases as d_2 increases, and increasing a_c will also enhance S_m.

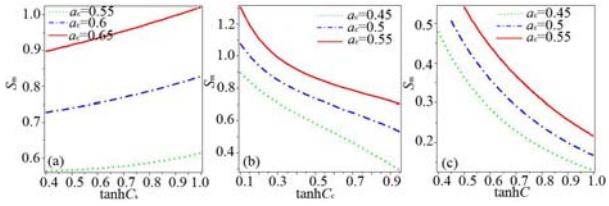

Fig. 7. (a) Sensitivity against tanhC_s for different values of a_c (a_s =0.8, a_m=-0.5, n=-0.6, d_1=300 nm, and d_2=80 nm); (b) Sensitivity against tanhC_c for different values of a_c (a_s =0.6, a_m=-0.5, n=-0.6, and d_1=200 nm, d_2=80 nm); (c) Sensitivity against tanh$C$ for different values of a_c (a_s =0.65, a_m=-0.5, n=-0.6, d_1=650 nm, and d_2=60 nm).

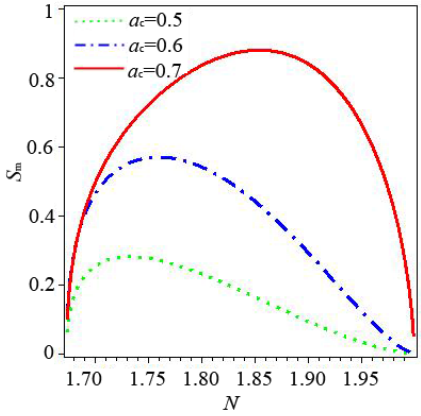

Fig. 8. Sensitivity versus the effective refractive index N for different values of a_c (a_s = 0.7, a_m=-0.5, n=-0.6, and d_2=80 nm).

Fig. 7 shows the relations between sensitivity and nonlinear parameters (tanhC_s, tanhC_c and tanh$C$). It is seen that S_m increases with increasing tanhC_s, and decreases with tanhC_c and tanh$C$. We can note in Fig. 7 (b) that the sensitivity S_m is larger than 1 in special case for TM mode, this phenomenon is in agreement with [14].

In Fig. 8, the sensitivity is plotted as a function of modal effective index N. It can be seen that the sensitivity is zero at N=1.673 (this value of N occurs at cut-off since it is equal to n_s, the figure is plotted for a_s = 0.7, $a_s = \varepsilon_s/\varepsilon_g$, and $n_s = \sqrt{\varepsilon_s}$) and at N=2 (this value of N is equal to the refractive index of guiding layer n_g). The sensitivity of the sensor increases with a_c. For different a_c, there exists an optimum value of N, with which the maximum sensitivity can be obtained.

S_m as a function of a_m the asymmetry parameter of the metamaterials is shown in Fig. 9. It can be seen that S_m increases with the decreasing absolute value of a_m.

It is seen from Fig. 10 that for both the normal symmetry case and the reverse symmetry case, S_m decreases with λ when d_1 is smaller than 150 nm; Contrarily, when d_1 is larger than 150 nm, S_m increases with λ. The insets show the magnetic field distribution along x axis for different λ when d_1=500 nm. It is seen that magnetic field increases with λ in the cladding layer. Therefore the variation of sensitivity coincides with the variation of magnetic field intensity. Thus wavelength λ is a determinant parameter for the guiding layer thickness at which the maximum sensitivity occurs.

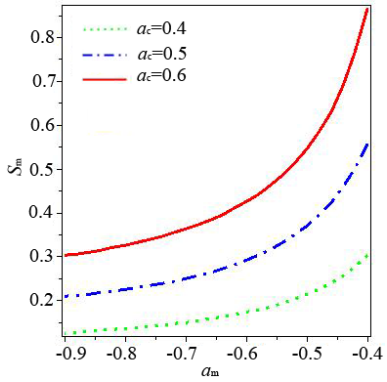

Fig. 9. Sensitivity against a_m for different values of a_c (a_s =0.72, a_m=-0.5, n=-0.6, d_1=400 nm, and d_2=60 nm).

According to the above investigation on sensitivity of the sensor, we compare the sensitivity as a function of the guiding layer thickness for four cases, as shown in Fig. 11. It can be seen from Fig. 11(a) that the maximum sensitivity of the proposed sensor is 2.335 times of that of the nonlinear planar optical waveguide sensor without metamaterials for TM mode. Fig. 11 (b) shows that when d_1 is below 370 nm, the sensor with linear cladding and substrate has the maximum sensitivity 0.905, when d_1 is above 370 nm, the sensitivity of the sensor with nonlinear cladding and substrate begins to surpass that of linear sensor; The sensitivity of the sensor in TM mode is much higher than that in TE mode when d_1 is greater than 80nm, as shown in Fig. 11 (c); The sensitivity of the sensor with reverse symmetry is higher than that with normal symmetry when d_1 is smaller than 280 nm (See Fig. 11 (d)), and the sensitivity of the sensor with reverse symmetry decreases with guiding layer thickness d_1 monotonously. We have also computed the sensitivity of the proposed sensor for TE mode. Results show that the maximum sensitivity of the proposed sensor for TE mode is 2.167 times for that without metamaterials, and is 1.167 times of that the metamaterial assisted linear planar optical waveguide sensor (details are not shown for brevity).

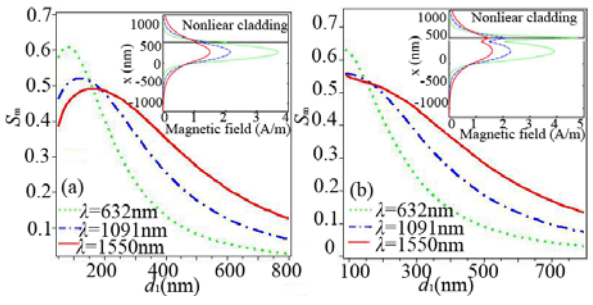

Fig. 10. Sensitivity against d_1 with different values of wavelength λ for the proposed waveguide (a_m=-0.5, n=-0.6, d_2=20 nm): (a) normal symmetry (a_s=0.51, a_c=0.5) (b) reverse symmetry (a_s=0.5, a_c=0.51).

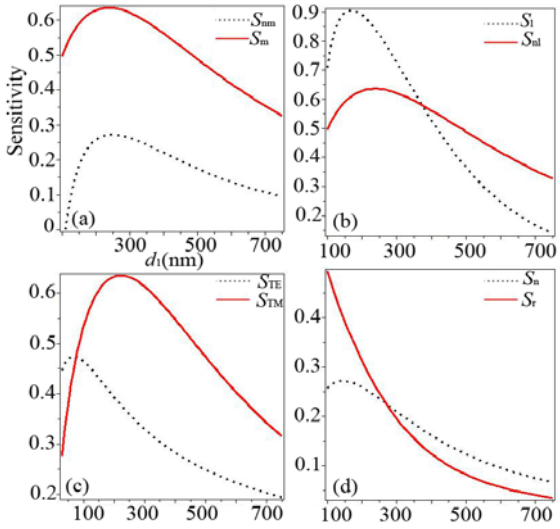

Fig. 11. Sensitivity against guiding layer thickness d_1 (a) with (a_s=0.65, a_c=0.55, a_m=-0.5, n=-0.6, d_2=65nm, nonlinear, TM mode, normal symmetry) and without metamaterials (a_s=0.65, a_c=0.55, nonlinear, TM mode, normal symmetry); (b) with linear (S_l) and nonlinear (S_{nl}) cladding and substrate (a_s=0.65, a_c=0.55, a_m=-0.5, n=-0.6, d_2=65nm, TM mode, normal symmetry); (c) for TE (S_{TE}) and TM (S_{TM}) mode (a_s=0.65, a_c=0.55, a_m=-0.5, n=-0.6, d_2=65 nm, nonlinear, normal symmetry) (d) with normal symmetry(S_n) (a_s=0.65, a_c=0.55, a_m=-0.5, n=-0.6, d_2=65 nm, nonlinear, TM mode) and reverse symmetry (S_r) (a_s = 0.55, a_c = 0.65, a_m = -0.5, n = -0.6, d_2=65 nm, nonlinear, TM mode).

4. Conclusions

We present a theoretical analysis of a nonlinear planar optical waveguide sensor loaded with a metamaterial layer, which includes deriving the dispersion relations of the waveguide, computing the magnetic field distribution of the waveguide, the sensitivity of the corresponding sensor, and the fraction of power flowing. The following conclusions are drawn from this study. Firstly, for both the TE and TM modes, evanescent wave can be amplified when the nonlinear planar optical waveguide is loaded with a layer of metamaterials. Secondly, the proposed metamaterial assisted nonlinear planar optical waveguide sensor possesses much higher sensitivity than the traditional nonlinear optical sensor. Besides, increasing the thickness of the metamaterial layer will further improve the performance of the proposed sensor. Thirdly, for TM mode the sensitivity of the proposed sensor is higher than the metamaterial assisted linear planar optical waveguide sensor when the guiding layer is thicker. Comparing TE with TM mode, the proposed sensor possesses much higher sensitivity when increasing the thickness of the guiding layer. Finally, the proposed sensor with reverse symmetry waveguide has higher sensitivity than that with normal symmetry waveguide when decreasing the thickness of the guiding layer. Generally, multiple factors

such as geometry parameters, transmission mode and dielectric characteristic of the waveguide influence the sensitivity of the sensor. Therefore, optimization design of the sensor is a key issue to achieve high sensitivity.

Acknowledgment

The authors would like to thank Dr. Taya (Physics Department, Islamic University, Palestinian) for helpful discussion. This work was supported by the National Natural Science Foundation of China (Grant Nos. 60861002, 61161007, 61162004), the Scientific Research Foundation of Yunnan University (Grant No. 2010YB025), and NSFC-YN (Grant No. U1037603).

References

[1] P. Andrew, W. L. Barnes, Science, **290**, 785 (2000).
[2] J. Wang, P. D. Coffey, M. J. Swann, F. Yang, J. R. Lu, X. Yang, Anal. Chem. **82**, 5455 (2010).
[3] J. Yang, L. Xu, W. Chen, Chin. Opt. Lett., **8**, 482 (2010).
[4] X. Dai, S. J. Mihailov, C. Blanchetière, Opt. Eng. **49**, 024401 (2010).
[5] J. Park, S. Lee, S. Kim, K. Oh, Opt. Express **19**, 1921 (2011).
[6] S. W. Phang, H. Z. Yang, S. W. Harun, H. Arof, H. Ahmad, J. Optoelectron. Adv. Mater. **13**, 604 (2011).
[7] J. Knittel, T. G. McRae, K. H. Lee, W. P. Bowen, Appl. Phys. Lett. **97**, 123704 (2010).
[8] R. Horvath, H.C. Pedersen, N. B. Larsen, Appl. Phys. Lett. **81**, 2166 (2002).
[9] S. P. Ng, C. M. L. Wu, S. Y. Wu, H. P. Ho, Opt. Express **19**, 4521 (2011).
[10] Z. Tian, S. S. H Yam, H. P. Loock, Opt. Lett. **33**, 1105 (2008).
[11] J. Cooper, A. Glidle, D. L. R. Richard, Opt. Photonics News 21, 26 (2010).
[12] J. Ang, H. C. H Li, I. Herszberg, M. K. Bannister, A. P. Mouritz, Int. J. Fatigue **32**, 762 (2010).
[13] R. Gao, N. Choi, S. I. Chang, S. H. Kang, J. M. Song, S. I. Cho, D. W. Lim, J. Choo, Anal. Chim. Acta **681**, 87 (2010).
[14] G. J. Veldhuis, O. Parriaux, H. J. W. M. Hoekstra, P. V. Lambeck, J. Lightwave Technol. **18**, 677 (2000).
[15] R. Abdurahman, A. Yimit, H. Ablat, M. Mahmut, J. D. Wang, K. Itoh, Anal. Chim. Acta **658**, 63 (2010).
[16] J. K. Seo, K. J. Kim, M. C. Oh, Opt. Commun. **283**, 1307 (2010).
[17] Y. Wang, C. J. Huang, U. Jonas, T. Wei, J. Dostalek, W. Knoll, Biosens. Bioelectron. **25**, 1663 (2010).
[18] M. Pu, L. Liu, H. Ou, K. Yvind, J. M. Hvam, Opt. Commun. **283**, 3678 (2010).
[19] L. Jin, M. Li, J. J. He, Opt. Lett. **36**, 1128 (2011).
[20] M. Huang, J. Yang, Microwave Sensor Using Metamaterials in: Wave Propagation, InTech Inc. Austria, 13 (2011).
[21] S. A. Taya, M. M. Shabat, H. M. Khalil, Optik **120**, 504 (2009).
[22] W. Niu, M. Huang, Z. Xiao, J. Yang, 9th International Symposium on Antennas, Propagation and EM Theory (ISAPE-2010), 2010 Beijing, 2010, p.697.
[23] S. A. Taya, M. M. Shabat, H. M. Khalil, D. S. Jager, Sens. Actuators A, Phys **147**, 137 (2008).
[24] D. Kumar, V. Singh, Optik - Int. J. Light Electron Opt. (2011), doi:10.1016/j.ijleo.2010.12.031.
[25] W. Niu, M. Huang, Z. Xiao, L. Zheng, J. Yang, Optik-Int. J. Light Electron Opt. (2011), doi:10.1016/j.ijleo.2011.05.022.
[26] R. Horváth, I. R. Lindvold, N. B. Larsen, Appl. Phys. B **74**, 383 (2002).

*Corresponding author: huangming@ynu.edu.cn